Large-scale responses of complex-shaped coastlines to local shoreline stabilization and climate change

Jordan M. Slott,[1] A. Brad Murray,[1] and Andrew D. Ashton[2]

Received 11 August 2009; revised 20 March 2010; accepted 2 April 2010; published 16 September 2010.

[1] When modeling the large-scale (> km) evolution of coastline morphology, the influence of natural forces is not the only consideration; ongoing direct human manipulations can substantially drive geomorphic change. In this paper, we couple a human component to a numerical model of large-scale coastline evolution, incorporating beach "nourishment" (periodically placing sand on the beach, also called "beach replenishment" or "beach fill"). Beach nourishment is the most prevalent means humans employ to alter the natural shoreline system in our case study, the Carolina coastline. Beach nourishment can cause shorelines adjacent to those that are nourished to shift both seaward and landward. When we further consider how changes to storm behaviors could change wave climates, the magnitude of morphological change induced by beach nourishment can rival that expected from sea level rise and affect the coast as far as tens of kilometers away from the nourishment site. In some instances, nonlocal processes governing large-scale cuspate-cape coastline evolution may transmit the human morphological "signal" over surprisingly large (hundreds of kilometer) distances.

Citation: Slott, J. M., A. B. Murray, and A. D. Ashton (2010), Large-scale responses of complex-shaped coastlines to local shoreline stabilization and climate change, *J. Geophys. Res.*, *115*, F03033, doi:10.1029/2009JF001486.

1. Introduction

[2] Geomorphologists have tended to study the dynamics of "pristine" systems, implicitly assuming that, to the first order, entirely "natural" (physical, chemical, biological) processes govern the shape of landscapes [e.g., *James and Marcus*, 2006]. Humans, however, play an ongoing, increasingly important role in directly shaping the Earth's surface. To support modern economies, entire landscape systems have been dramatically altered from their previous pristine state (e.g., the lower Colorado River and the lower Mississippi River Delta basins). By some measures, humans are responsible for mobilizing more sediment each year than any other "natural" force [*Hooke*, 1994, 2000]. Understanding how landscape systems will evolve over the coming centuries, however, necessitates including humans as a first-order agent of change [*Haff*, 2007].

[3] Coastlines provide a stark example of this recent trend in landscape morphodynamics. Humans are now an integral part of how many coastlines evolve, resulting in a fundamentally different system from that which existed before humans and their technology effected such dramatic change [*McNamara and Werner*, 2008a, 2008b; *Syvitski et al.*, 2005; *Werner and McNamara*, 2007]. In response to the shifting position of the shoreline, humans are likely to prevent landward retreat in some places, effectively "pinning" the shoreline position and arresting its natural dynamic tendency. Beach "nourishment," in which sand is typically dredged from offshore and placed on a section of landward-retreating beach (also called "beach fill"), has become the predominant stabilization method on many coastlines.

[4] To understand how the morphology of coastlines naturally evolve, scientists have previously developed many different numerical modeling frameworks that focus on a range of spatial and temporal scales [*Ashton and Murray*, 2006a; *Hanson and Kraus*, 1989; *Larson et al.*, 1990; *Reolvink and Van Banning*, 1994]. The inputs that drive these models typically include wave-driven currents and sediment transport, tides, and sea level rise. One specific class of these models ("one-contour-line" models) assume the cross-shore profile of the nearshore seabed remains constant over time [*Dean*, 1991]; they address the landward or seaward shifts of wave-dominated, sedimentary coastlines that result from gradients in alongshore sediment transport. These numerical modeling efforts, where the shoreline evolves freely in response to natural forces (including climate change), may not be applicable to developed shorelines, however. Previous attempts at modeling human manipulations (e.g., beach nourishment) to the shoreline, such as GENESIS [*Hanson and Kraus*, 1989], treat site-specific and relatively short-term (years) effects and are not suited to studying the evolution of large-scale, complex coastlines.

[5] We extend a numerical model of shoreline change that has been recently developed to explore coastline evolution on large spatial scales (one to hundreds of kilometers) and

[1]Division of Earth and Ocean Sciences, Nicholas School for the Environment and Earth Sciences, Center for Nonlinear and Complex Systems, Duke University, Durham, North Carolina, USA.
[2]Geology and Geophysics Department, Woods Hole Oceanographic Institution, Woods Hole, Massachusetts, USA.

0148-0227/10/2009JF001486

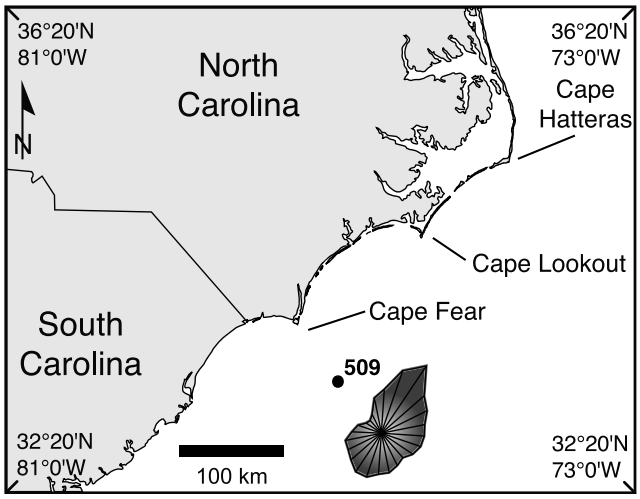

Figure 1. The coastline of North Carolina and South Carolina, from Cape Hatteras, NC, to Cape Fear, SC, along the U.S. Atlantic coastline. From *Ashton and Murray* [2006b].

long time scales (years to centuries) [*Ashton and Murray*, 2006a] to include beach nourishment. We report on a series of model experiments involving both a smooth coastline and a cuspate-cape coastline similar to the Carolina capes, from Cape Hatteras, North Carolina, to Cape Fear, South Carolina, USA (Figure 1). The Carolina capes represent an important case study: they are a prominent example of a developed coastline, and one with a relatively long history of beach nourishment [*Pilkey et al.*, 1998; *Valverde et al.*, 1999]. In this work, however, we do not intend to produce quantitative predictions about the future of a specific shoreline to be used in an engineering context; rather, we are trying to understand the large-scale, long-term evolution of a complex-shaped coastline where human interaction plays an integral part of the system.

2. Background

2.1. High-Angle Wave Instability

[6] The magnitude of alongshore sediment transport is a function of the relative angle between deepwater wave crests (before nearshore shoaling and refraction) and the local shoreline orientation (Figure 2a). Alongshore flux exhibits a maximum when this deepwater relative angle approximately equals 45°, assuming shore-parallel contours extend to deep water from perturbations to the plan view shoreline [*Ashton et al.*, 2001; *Ashton and Murray*, 2006a; *Falqués and Calvete*, 2005; *List and Ashton*, 2007; *Deigaard et al.*, 1988].

[7] Waves that approach the shoreline from relative angles greater than the flux-maximizing angle (~45°) or "high-angle" waves induce instabilities in the shoreline shape; they cause plan view perturbations to grow seaward [*Ashton et al.*, 2001; *Ashton and Murray*, 2006a] (Figure 2b). Low-angle waves (<~45°), on the other hand, smooth plan view shoreline shapes (Figure 2c). When a wave climate features a greater influence from high-angle than low-angle waves, subtle plan view shoreline bumps will grow seaward over time (antidiffusion) [*Ashton et al.*, 2001; *Ashton and Murray*, 2006a, 2006b; *Falqués and Calvete*, 2005]. Conversely, when low-angle waves have a greater influence than high-angle waves in a wave climate, alongshore sediment transport tends to diffuse plan view shoreline perturbations.

[8] *Ashton et al.* [2001] showed how hundred kilometer scale complex plan view coastline patterns, such as the cuspate-cape coastline of the Carolinas (Figure 1), can self-organize from an initially straight, slightly rough shoreline over geologic time (millennia). In their model experiments, capes grow seaward because the directional wave climate they use contained proportionally more high-angle waves (and waves approaching equally, or nearly so, from the left and right). Their model also incorporated "wave shadowing," where protruding sections of coastline may physically block certain approaching waves that would otherwise reach adjacent sections of coastline. As plan view shoreline perturbations grow into capes, some extend farther seaward than their neighbors and therefore shadow their neighbors from waves approaching from the highest angles (that have the greatest antidiffusive influence) [*Ashton and Murray*, 2006a]. The more-often shadowed capes, feeling fewer high-angle waves, experience a relative decrease in their cross-shore extent, which increases their shadowing. Although the regional wave climate remains antidiffusive, the "local wave climate" of the smaller capes eventually becomes diffusive. Thus, a smaller cape eventually disappears, leaving a smaller number of larger capes over time. Wave shadowing therefore appears to play a key role in cuspate-cape shoreline evolution, allowing capes to directly interact with one another over surprisingly large distances (tens to hundreds of kilometers) [*Ashton and Murray*, 2006b].

2.2. Sensitivity of a Cuspate-Cape System to Shifting Wave Climates

[9] Using a modeling approach similar to *Ashton et al.* [2001], *Slott et al.* [2006] explored how an existing, complex coastline shape shifts on human time scales (decades to centuries) if the distribution of wave influences from different deepwater wave approach directions changes. This case study addressed the cuspate-cape coastline of North Carolina and South Carolina, where roughly 125 km separates each cape (Figure 1). The wave climate influencing this stretch of coastline is dominated by waves that approach from the northeast and from the southwest, generated by a combination of extratropical and tropical storms and prevailing winds. As a result, waves approach the Carolina coast predominately from high angles, with slightly more influence from waves from the northeast [*Ashton and Murray*, 2006b]. The Carolina capes have presumably recently existed in a quasi-equilibrium state with this wave climate as the cuspate-cape system has migrated southwestward over the past half-century (50 year historical shoreline data can be found at http://dcm2.enr.state.nc.us/Maps/erosion.htm, hereafter *NC50*).

[10] Changes in the relative frequency and/or magnitude of storms would alter the directional distribution of wave influences felt by the Carolina coast. Increased tropical storm intensity is one possible outcome of global warming and increased sea surface temperatures (SSTs) [*Emanuel*, 1987, 2005]. *Slott et al.* [2006] found that moderate shifts in storminess patterns and the subsequent effect on wave climates could increase the alongshore-averaged rate at which the shoreline recedes or accretes (the average magnitude of the shoreline change rate) to at least several times

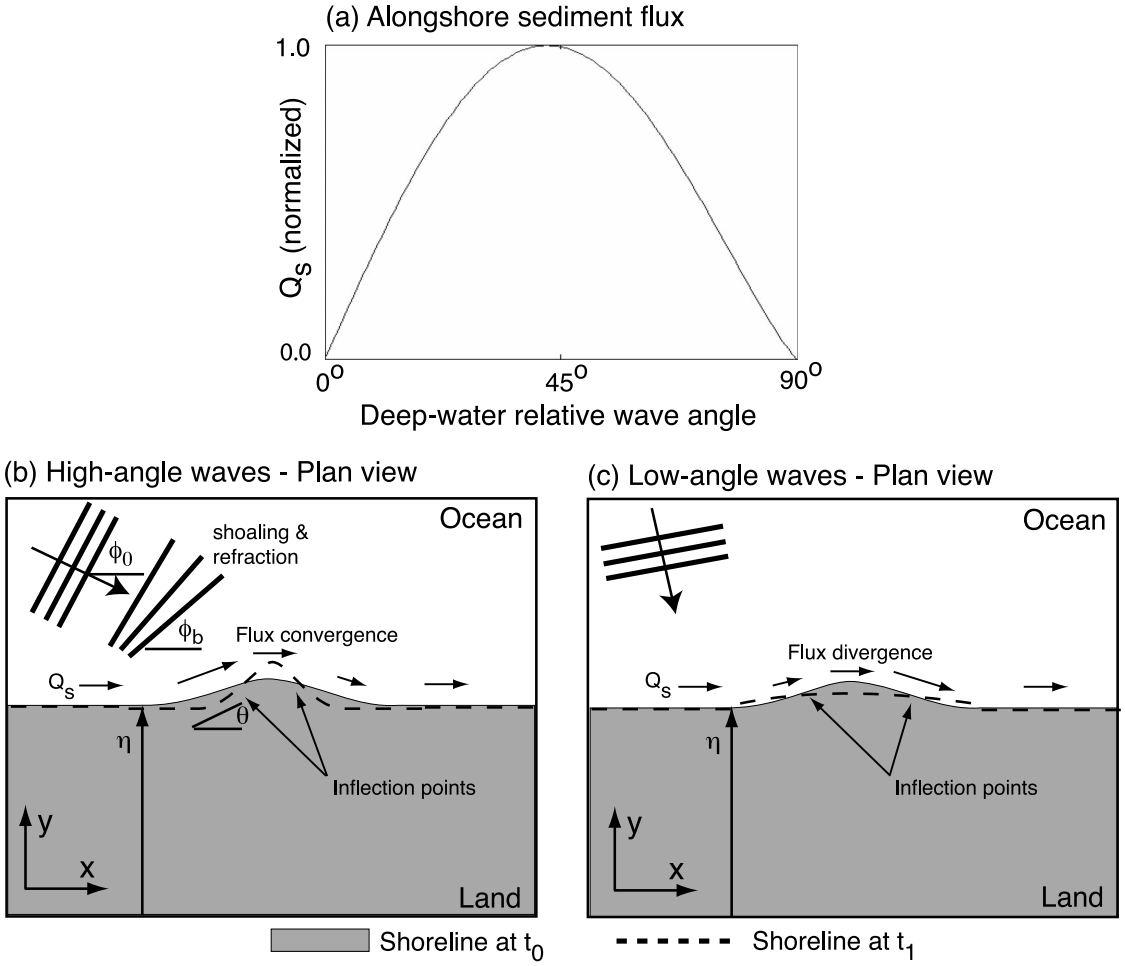

Figure 2. Schematic illustration of zones of shoreline recession and accretion caused by gradients in the alongshore sediment flux Q_s. (a) Plot of alongshore sediment flux Q_s as a function of the relative angle between deepwater wave crests and the shoreline. Alongshore sediment transport is maximized for relative deepwater wave angles of ~45°. (b) Growth of a shoreline bump caused by a convergence in Q_s along the bump crest (magnitudes depicted by varying-length arrows) when subjected to high-angle waves. ϕ_o is the deepwater wave approach angle, ϕ_b is the breaking wave angle, and θ is the shoreline angle. (c) Smoothing caused by a divergence of alongshore sediment transport on the crest of a shoreline bump when subjected to low-angle waves. After *Slott et al.* [2006].

the recent historic rate of shoreline change, an effect greater than the recession we expect from sea level rise alone over the coming century [*Intergovernmental Panel on Climate Change*, 2007; *Moore et al.*, 2007, *Wolinsky and Murray*, 2009]. Shoreline segments near the cape tips experienced the greatest rates of shoreline recession or accretion in these model results, exceeding the present alongshore-averaged change rates by up to an order of magnitude. The coastline change analysis performed by *Slott et al.* [2006], however, ignored the effect that human shoreline stabilization practices will have (practices which will likely become more prevalent if typical rates of shoreline change accelerate).

2.3. Beach Nourishment

[11] Other "one-contour-line" models of the plan view evolution of shorelines treat beach nourishment as small perturbations to the regional shoreline orientation [*Dean*, 2002; *Hanson and Kraus*, 1989]. They further assume that waves approach either directly from offshore or slightly askew. For example, *Dean and Yoo* [1992] subject shorelines to waves approaching from a maximum 20° from the shore normal. As a result, the plan view perturbations to the shoreline caused by beach nourishment are smoothed out, and adjacent beaches advance seaward, the long-studied diffusion of shoreline shape [*Dean and Yoo*, 1992; *Dean*, 2002].

[12] These models, which typically consider the site-specific and relatively short-term (years) effects of beach nourishment [e.g., *Dean and Yoo*, 1992; *Dean*, 2002; *Hanson and Kraus*, 1989], do not consider beach nourishment in the context of recent advances in the understanding of large-scale coastline morphodynamics: they do not consider waves approaching the shoreline from highly oblique angles nor the instability they induce in plan view shoreline shape; they do not consider shorelines situated within a larger, complex-shaped coastline; and they do not

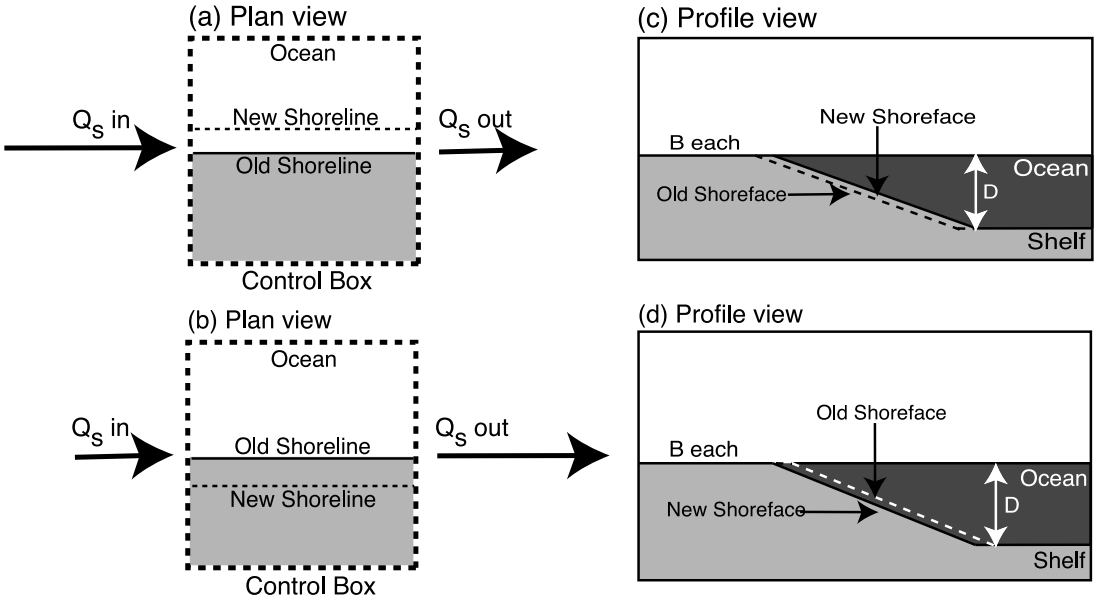

Figure 3. "One-contour-line" modeling approach. Gradients in alongshore sediment transport (Q_s) cause (a) accretion from a convergence in alongshore sediment transport flux and (b) recession from a divergence in alongshore sediment transport flux. (c) During accretion, the entire cross-shore profile, represented here as linear, shifts seaward. (d) During recession, the entire cross-shore profile shifts landward. (For the purposes of a one-contour-line model, the shape of the nearshore profile is irrelevant if it does not change over time; the depth to which recession or accretion extends D affects model rates.) After *Slott et al.* [2006].

consider wave climate shifts resulting from climate change. In this paper, we consider large-scale coastline evolution, as influenced by beach nourishment, in these three contexts.

3. Methods

3.1. Numerical Model

[13] The numerical model we use is described in detail elsewhere [*Ashton and Murray*, 2006a], and here we recapitulate only the main points. A continuity equation describes shoreline evolution in our one-contour-line numerical model,

$$\frac{\partial \eta(x,t)}{\partial t} = -\frac{1}{D}\frac{\partial Q_s(x,t)}{\partial x}, \tag{1}$$

where η is the cross-shore shoreline position, x is the alongshore coordinate (Figure 2), Q_s is the alongshore sediment flux (m^3/d), and D is the water depth (m) to which cross-shore wave-driven transport processes redistribute sediment over the seabed (Figure 3).

[14] Our model discretizes the continuity equation in time and space by dividing the plan view shoreline into a two-dimensional grid of cells. Shorelines are allowed to form complex shapes such as capes and spits; the model defines local coordinate systems for each model cell based upon its local shoreline orientation when computing alongshore transport volumes. The model employs alongshore periodic boundary conditions. For cells shadowed by other coastline features, the model sets alongshore sediment flux to zero.

[15] The model refracts and shoals deepwater waves over assumed shore-parallel contours until breaking occurs [*Komar*, 1998]. *Falqués and Calvete* [2005] relax this constraint, additionally consider combinations of wave parameters (period, deepwater wave height) and shoreface geometry (active profile depth, wave-breaking depth), and found that for shorelines with undulations of sufficiently large alongshore wavelength (>~10 km), the high-angle wave instability mechanism holds over a robust set of wave and shoreface parameters [*Falqués and Calvete*, 2005].

[16] We use the common CERC (Coastal Engineering Research Center) formula to compute alongshore sediment transport as a function of the significant breaking wave height, the breaking wave angle, and the local shoreline angle,

$$Q_s = KH_b^{5/2}\sin(\phi_b - \theta)\cos(\phi_b - \theta), \tag{2}$$

where H_b is the root mean square breaking wave height, ϕ_b is the breaking wave angle, and θ is the local shoreline angle (Figure 2). K is an empirical constant with a high degree of variability and uncertainty [*Komar*, 1971, 1998; *Komar and Inman*, 1970]. Although K, which depends upon a host of factors (e.g., sediment grain size), can vary widely on different shorelines, we assume it remains constant across the model domain. Although a value of $K = 0.17\ m^{1/2}/s$ is often used based upon a fit to previous measurements [*Komar*, 1998], we selected a K of $0.4\ m^{1/2}/s$. This value was attained by calibrating model shoreline changes to 50 years of historical shoreline change along the outer banks of North Carolina [*NC50*; *Slott et al.*, 2006], using recent wave climate conditions (WIS Station 509, see Figure 1) (WIS data can be found at http://frf.usace.army.mil/wis/, hereafter *WIS*) and a value of 10 m for D chosen to match conditions that exist on our case study coastline [*USACE*, 2002].

3.2. Wave Selection in Model Experiments

[17] Our numerical model randomly selects a new incoming deepwater wave angle each simulated day from a probability distribution function (PDF) of wave approach angles. The PDF is described by two parameters, A and U. The wave asymmetry parameter A gives the probability that a wave will approach from the left, looking offshore. The wave highness parameter U gives the probability that a wave will approach from a high angle (>45°). The deepwater wave height is kept fixed for all wave approach angle selections.

[18] This simplified representation of the wave climate using these two parameters makes clear the relationship between coastline behavior and the angular distribution of approaching waves: wave climates featuring values of A greater than (less than) 0.50 result in net alongshore sediment transport to the right (left), looking offshore, and wave climates featuring values of U greater than (less than) approximately 0.50 result in the growth (diffusion) of shoreline "bumps."

3.3. Beach Nourishment

[19] During any time step in which the shoreline in a reach designated as a nourishment area erodes beyond its original position, we add sand to bring the shoreline back to its original position. Beach nourishment therefore compensates for an imposed recession of the coastline or divergences in wave-driven alongshore sediment transport by adding sand to the shoreline system. We assume any sand added to the shoreline, whether from terrestrial or underwater sources, is taken from areas entirely external to the modeled shoreline system. The model does not prevent the nourished area of the shoreline from accreting through gradients in alongshore flux nor does it add additional nourishment sand in these cases. During the model run, we track the total volume of sediment placed on the beach by nourishment as the product of the cross-shore width of shoreline added, the alongshore length of the beach nourishment site (10 km) and the depth to which sand spreads out over the shoreface (Figure 3d).

[20] In the real world, sand is placed on the subaerial beach and in and near the swash and surf zones during beach nourishment. This placement disturbs the cross-shore equilibrium profile. Cross-shore processes then redistribute some of that nourishment sand out over the active shoreface, tending to restore the cross-shore profile to its equilibrium shape. The redistributive process occurs on the time scale of months to several years [*Dean*, 2002]. We do not explicitly include the transient, disequilibrium state immediately following beach nourishment because our time scales of interest (decades to centuries) are much larger than the inherent time scale of this transient behavior (months to years). This exploratory model treats beach nourishment as if the sand immediately spreads over the active shoreface.

4. Model Experiment 1: Nourishment of a Flat Shoreline

4.1. Description of Model Experiment

[21] We first consider the long-term effects of beach nourishment on the evolution of a straight shoreline and compare these basic results to the traditional diffusion model of shoreline evolution [*Dean and Yoo*, 1992; *Dean*, 2002]. Rather than nourish a section of beach once, we consistently nourish a 10 km segment of beach over a 200 year model run, representing a town's policy to stabilize the position of its beach over the long term. In each of six experiments, we choose a different wave climate where waves approach the coastline either equally from the left and right (A = 0.5) (Figure 4a) or 70% from the left, looking offshore (A = 0.7) (Figure 4b), while the proportion of waves approaching from high angle is either U = 0.0 (entirely diffusive), U = 0.3, or U = 0.5 (borderline neutrally diffusive). In these experiments, we impose a 1 m/yr, uniform recession rate across the entire shoreline.

4.2. Results

[22] When U = {0.0, 0.3}, the effects of beach nourishment diffusive laterally and advance adjacent beaches, as demonstrated by *Dean and Yoo* [1992]. Also, similar to results by *Dean and Yoo* [1992], the diffusive effects were insensitive to the directional asymmetry of the wave climate in these cases. It is important to note, however, that despite commonly held notions the mechanisms causing adjacent beaches to advance differ between the A = 0.5 and A = 0.7 cases. When A = 0.5, sediment flux is directed leftward toward the neighboring beach to the left and rightward toward the neighboring beach to the right: sand spreads from the nourishment area in both directions (Figure 4c).

[23] When A = 0.7, however, net sediment flux is directed rightward: the beach to the left of the nourishment area advances because gradients in the rightward-directed flux due to the nourishment cause sand to accumulate updrift of the nourishment site and not because sediment spreads leftward from the nourishment area (Figure 4d). Contrary to popular misconceptions, neighboring beaches can benefit from nourishment even if sand does not "leak" from a nourishment area. Beach nourishment pins the shoreline segment in place, not allowing it to evolve in response to natural forcings, and alters the angle the nourished area makes with the unnourished, adjacent shoreline segment. We further examine the shoreline orientation effect in section 6.3.5.

[24] Under an asymmetric wave climate (A = 0.7), when the wave climate is no longer definitively weighted toward low-angle waves (e.g., U = 0.5), the effects of beach nourishment no longer spread uniformly in each direction, and the directional asymmetry of the wave climate plays a stronger role in determining the nature of shoreline evolution. This case also demonstrates an unexpected result: adjacent beaches may wind up landward of their initial position because of the nourishment (Figures 4a and 4b) because of shadowing and shoreline orientation effects (see section 6.3.5). The effects of beach nourishment diffuse laterally to a greater extent and are felt on stretches of beach farther away from the nourishment area for smaller values of U than for larger values of U even though the wave height (and therefore, the wave energy) across each of these wave climates remains the same.

5. Model Experiment 2: Nourishment on a Cuspate-Cape Shoreline

5.1. Description of Model Experiment

[25] On complex-shaped coastlines such as the cuspate-cape system resembling the Carolina coastline (Figure 1),

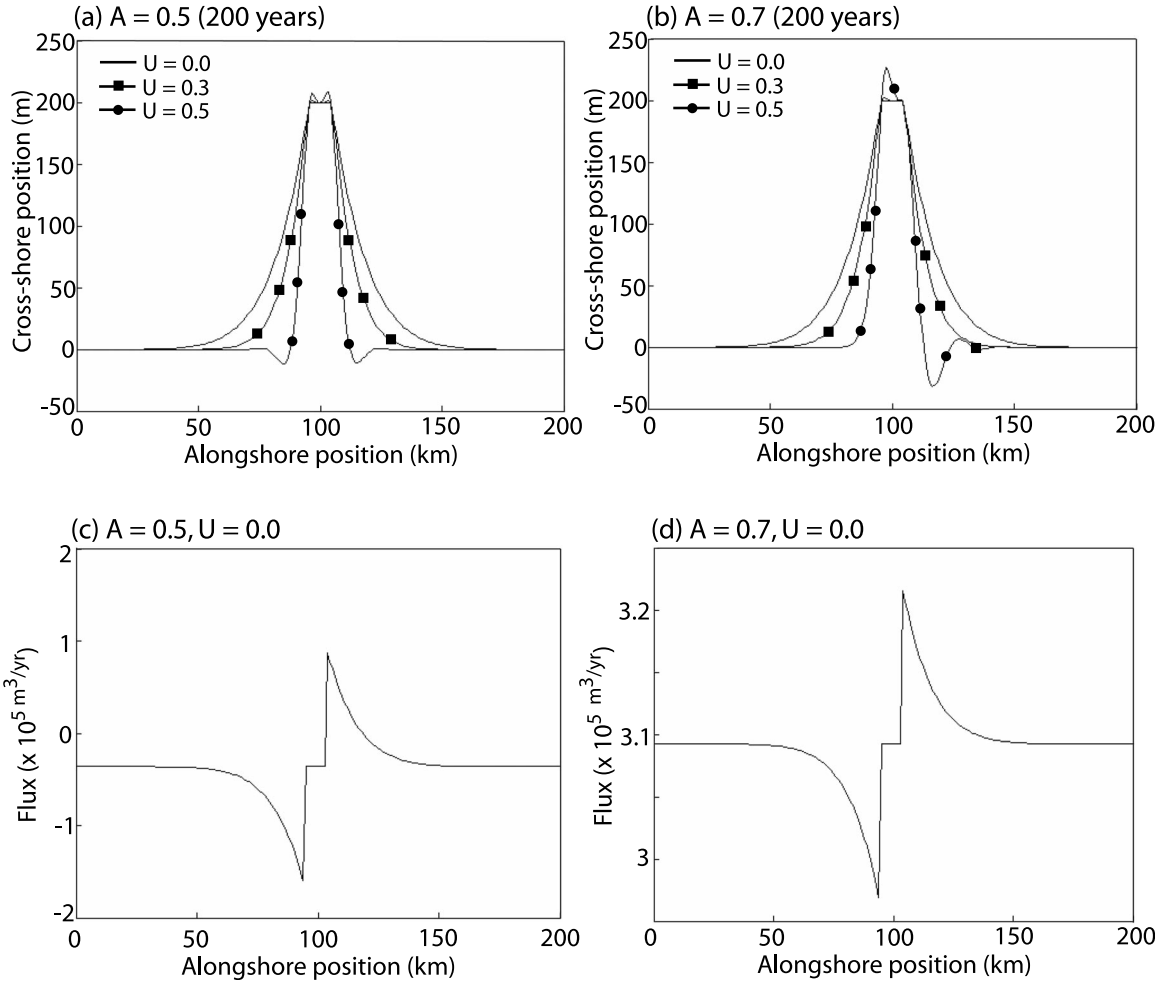

Figure 4. Evolution of a flat shoreline in response to repeated beach nourishment over 200 years under an imposed baseline recession rate of 1 m/yr. (a) Shoreline position relative to baseline recession under symmetric wave climates (A = 0.50) with varying influences from high-angle waves (U = { 0.0, 0.3, 0.5}). (b) Shoreline position relative to baseline recession under asymmetric wave climates (A = 0.70) with varying influences from high-angle waves (U = {0.0, 0.3, 0.5}). (c) Plot of time-averaged flux per alongshore position for model simulation from Figure 4a, where U = 0.0. (d) Plot of time-averaged flux per alongshore position for model simulation from Figure 4b, where U = 0.0. Positive flux values are directed rightward in Figures 4c and 4d, looking offshore.

stretches of shoreline may be considered "smooth" locally (one to tens of kilometers alongshore scale), but they are typically situated within a larger context. For example, the shoreline along each Carolina cape flank is rotated with respect to the regional northeast to southwest trend of the cuspate-cape system. The wave climate felt locally on these stretches of shoreline depend upon the regional wave climate and on the different shoreline orientations. The wave climate local to each shoreline is also affected by how waves are blocked by protruding plan view features (wave shadowing) [*Ashton and Murray*, 2006a, 2006b]. We now explore how local shoreline orientation and wave shadowing interact with beach nourishment to influence coastline evolution in a series of 200 year model runs where we vary the alongshore position of a 10 km nourishment site across a cuspate-cape system.

5.2. Wave Climate

[26] We expose the initial cuspate-cape model shoreline to a wave climate resembling current conditions off of the U.S. East Coast with 20 years of wave hindcast data computed for a location off of the Carolina coast (WIS Station 509, see Figure 1). To weight the wave climate parameters A and U based upon the wave hindcast data, we first recast equation (2) in terms of deepwater quantities [*Ashton et al.*, 2001],

$$Q_s = K_2 H_0^{12/5} \sin(\phi_0 - \theta) \cos^{6/5}(\phi_0 - \theta), \quad (3)$$

where H_o is the deepwater wave height, ϕ_o is the deepwater wave approach angle (Figure 2), and K_2 is an empirical constant equal to 0.32 $m^{3/5}$ $s^{-6/5}$. From equation (3), we observe that alongshore sediment transport scales

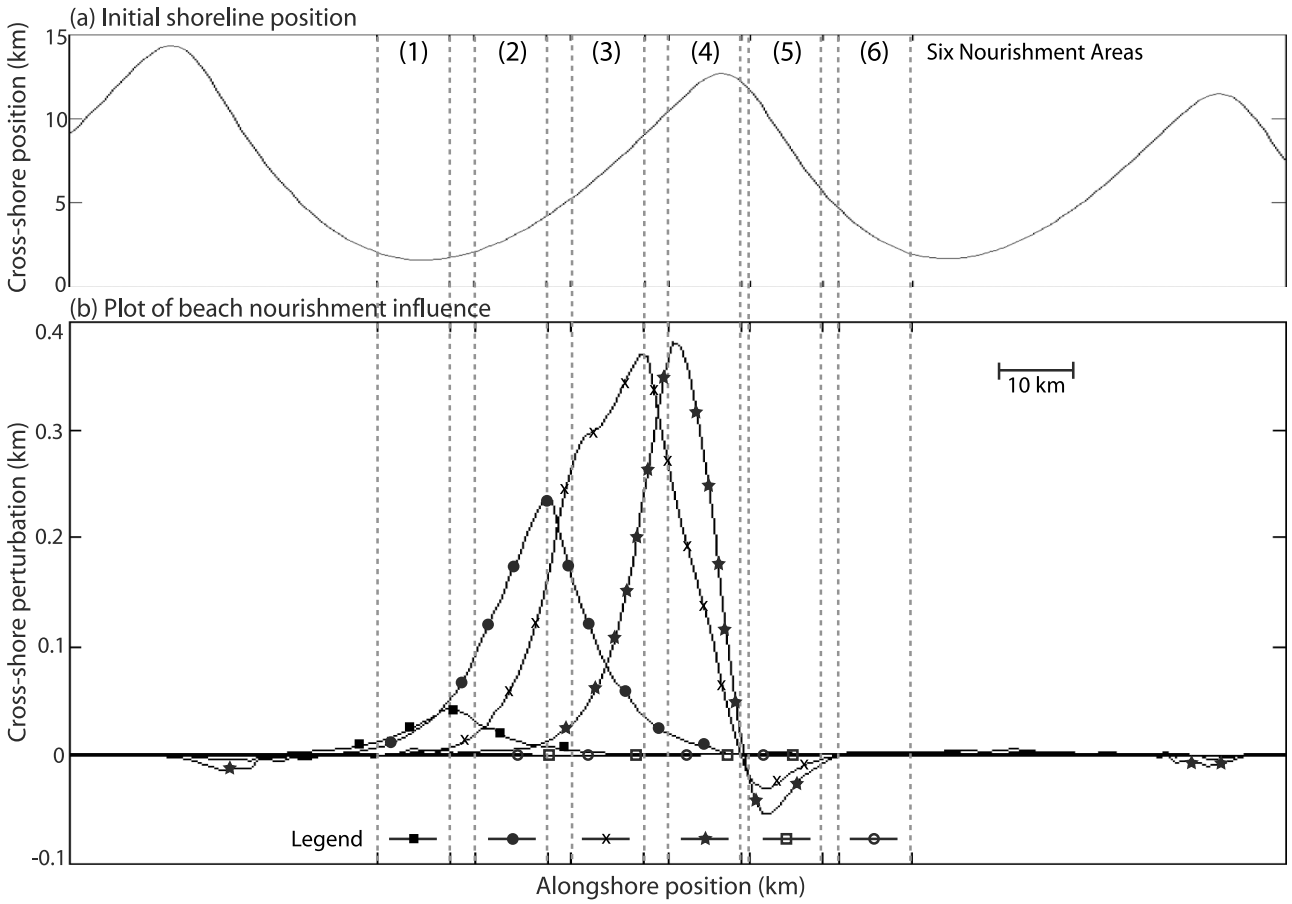

Figure 5. Evolution of a cuspate-cape shoreline in response to repeated beach nourishment over 200 years for six different site selections, subjected to a wave climate approximating recent conditions off of the Carolina coast (WIS). (a) Plot of initial model shoreline position. (b) Plot of the influence beach nourishment at six different areas had on shoreline evolution, normalized for the cuspate-cape shape of the shoreline and the extent to which it naturally migrated under natural wave forces. (c) Cumulative beach nourishment volume (m^3) for model runs.

with deepwater wave height raised to the 12/5 power; we scale the contribution to the PDF of each wave from the wave hindcast data similarly (e.g., storm waves, with larger wave heights, contribute more weight to their wave approach angle bin than do smaller waves). The deepwater significant wave height is held constant throughout the model run at 1.7 m, computed as $< H_0^{12/5} >^{5/12}$ [*Slott et al.*, 2006]. A loose fit to our simplified four-bin wave climate to the data from WIS Station 509 (*WIS*) yields $A = 0.55$ and $U = 0.60$ [*Ashton and Murray*, 2006b]. While equation (3) is employed to compute the two wave climate parameters, A and U, from the WIS wave data, during model runs, waves selected using these wave climate parameters are shoaled and refracted over shore-parallel contours, and equation (2) is applied to compute the alongshore sediment flux.

5.3. Initial Model Condition

[27] We generated our initial 900 km cuspate-cape model shoreline by subjecting a straight shoreline with hundred meter white noise perturbations to waves selected from the PDF representing recent wave climate conditions (*WIS*, 1980–1999). After ~8000 simulated years, the shoreline exhibits capes spaced ~60–100 km apart. The capes have an aspect ratio of ~5–6, roughly approximating the cuspate-cape system of the North and South Carolina coastline featuring capes spaced ~125 km apart. We also conducted a set of representative model experiments using a shoreline featuring capes spaced ~125 km apart generated from a 20,000 simulated year run using recent wave climate conditions (*WIS*). After calibrating the rates of change in the model to 50 years of historical shoreline data [*NC50*; *Slott et al.*, 2006], these model runs showed the same patterns of

seaward and landward shoreline shifts nearly identical in magnitude to the experimental results shown in this paper. (We do not mean to simulate the Holocene evolution of the Carolina coastline in detail; in all likelihood undulations existed in the shoreline when Holocene sea level rise slowed down. Furthermore, the 20 year WIS hindcast data is not an accurate representation of the wave climate over the past 8000 years. Our initial model shoreline is only an abstract representation of the Carolina coast.)

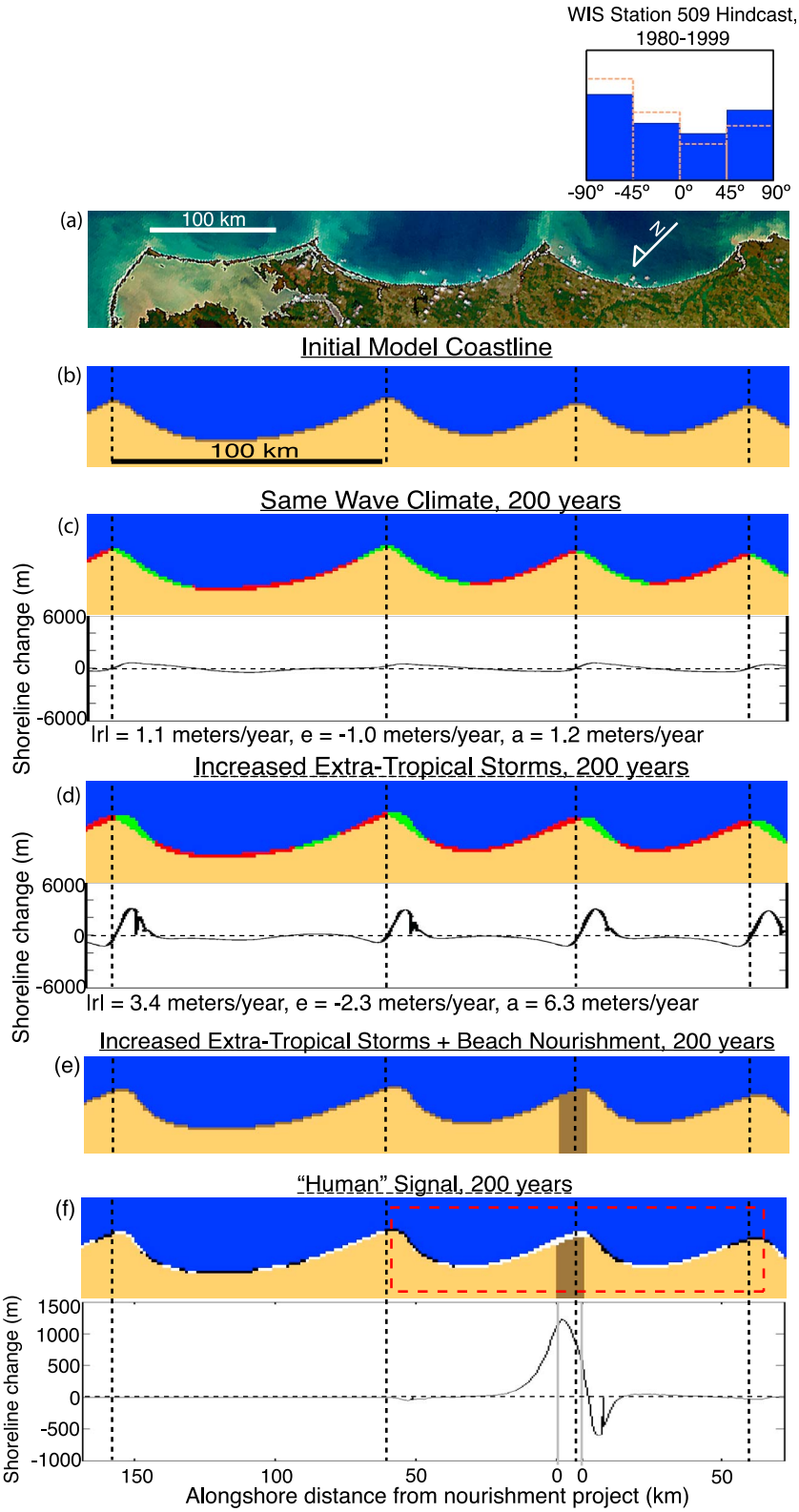

Figure 6

5.4. Results

[28] We plot the position of the shoreline after 200 years for each run, normalized for the shape of the shoreline and the extent to which shoreline position migrated under natural forces (Figure 5). This is performed as follows: in addition to each model experiment where we nourish a section of beach, we conduct a "control" run without beach nourishment, using the identical initial condition and wave climate (as if it existed in a parallel universe). We subtract the position of the shoreline after 200 years in model runs with beach nourishment from the control model run to derive the "human" component of the coastline evolution signal.

[29] We observe dramatically different large-scale coastline responses depending upon the location of beach nourishment. Shoreline changes caused by nourishment at locations near the center of the cuspate bay (Figure 5b, (1) and (2)) resembles the classic diffusion of shoreline shape; local wave climates here are weighted toward low-angle waves as the protruding capes tend to block the high-angle wave component of the regional wave climate [*Ashton and Murray*, 2006b]. As the beach nourishment location approaches the tip of a cape where the influence of wave shadowing is diminished, shoreline evolution exhibits the asymmetric character of earlier experiments where flat shorelines were exposed to roughly equal influences from high-angle and low-angle waves (Figure 5b, (3) and (4)). Nourishment at the tip of the cape (Figure 5b, (4)) pins the cape in its initial position, alters the angle the shoreline makes with its adjacent unnourished segment, and induces an ~50 m landward shift (relative to the nonnourishment control) of the adjacent downdrift beach over 200 years. Nourishing at the tip of the cape (Figure 5b, (4)) also reveals the nonlocal way in which the "human" signal of geomorphic change is transmitted to distant shorelines: noticeable perturbations to shoreline evolution are visible on adjacent cape flanks, although the magnitude of these perturbations are small compared to other affected stretches of the shoreline. We explore the last scenario (Figure 5b, (4)) further when we consider global warming–induced changes in wave climates below.

[30] The extent to which beach nourishment–influenced shoreline evolution over the long term depends, in part, upon how wave-driven alongshore sediment transport governs patterns of recession and accretion. On our cuspate-cape shoreline, capes naturally migrate rightward (looking offshore) in response to the slightly asymmetric regional wave climate. Areas that experience high rates of naturally induced shoreline recession (i.e., to the left of cape tips) experience the largest influences from beach nourishment (e.g., Figure 5b, (1) through (4)) and the greatest requirements for beach nourishment activity (Figure 5c). Accreting areas experience the smallest influence from beach nourishment (Figure 5b, (5) and (6), the influence is imperceptible) and the smallest requirements for beach nourishment activity (Figure 5c).

6. Model Experiment 3: Nourishment on a Cuspate-Cape Coastline Under Altered Wave Climates

6.1. Description of Model Experiment

[31] The model experiments above considering the long-term effect of beach nourishment on the evolution of a cuspate-cape shoreline have not involved changing wave climates. Moderate changes in the relative distribution of wave influences on alongshore sediment transport can result in substantially altered patterns of shoreline recession and accretion [*Slott et al.*, 2006].

6.2. Wave Climate

[32] As in the work of *Slott et al.* [2006], we represent global warming–induced changes to storm patterns through scenarios involving shifts in wave climate conditions. In these scenarios, the relative influence from tropical storms may increase, the relative influence from extratropical storms may increase, or the relative influence from prevailing winds may increase (e.g., representing a relative decrease in storminess). For example, waves from extratropical storms generally approach the southeast U.S. coastline from the northeast, so that in a scenario representing increased strength of such storms, the relative contribution of these waves to alongshore transport increases. In wave climate change scenarios, we vary the directional wave asymmetry parameter (A) and the wave angle highness parameter (U) accordingly. We approximate the magnitude of changes in A

Figure 6. Shoreline response to increased extratropical storm influence and a 10 km beach nourishment. (a) The cuspate-cape shoreline of the Carolinas, rotated 150° counterclockwise so that the normal to the regional shoreline trend points up. Satellite image courtesy of the SeaWiFS Project NASA/GSFC and ORBIMAGE. (b) An initial model condition, generated using the approximation to the WIS wave climate data (blue in inset), resembling the Carolina capes. (c) The cuspate-cape initial model condition subjected to 200 years of waves drawn from a PDF of wave hindcasts based on WIS Station 509 (*WIS*) (A = 0.55, U = 0.60, blue in inset). Shoreline change over 200 years is depicted graphically and summarized by $|r|$, the alongshore average of the magnitude of shoreline change, by e, the alongshore average of recession in receeding areas, and by a, the alongshore average of accretion in accreting areas. (d) The cuspate-cape shoreline subjected to 200 years of waves drawn from a wave climate featuring a greater portion of waves approaching from the left (A = 0.65), representing an increase in the influence of extratropical storms (dotted rectangles in inset). Green shoreline segments represent zones of accretion, and red segments represent zones of recession. Shoreline change over 200 years is depicted graphically. (e) An altered cuspate-cape shoreline subjected to 200 years of waves drawn from a wave climate featuring a greater portion of waves approaching from the left (A = 0.65, U = 0.60, inset), representing an increase in the influence of extratropical storms, and a 10 km beach nourishment located near the tip of one cape. (f) The change in shoreline position between Figures 6d and 6e due solely to the 10 km beach nourishment. (The red-colored rectangle denotes the region analyzed further in Figure 10.) After *Slott et al.* [2006].

and U equals roughly 0.10, obtained using estimates of the expected increase in tropical storm intensity over the coming century [*Slott et al.*, 2006].

[33] In the results presented here concerning the influence of beach nourishment on a cuspate-cape coastline under climate change scenarios, we focus on model experiments using a single altered wave climate featuring an increase in extratropical storm-generated waves (A = 0.65 and U = 0.60). We selected this wave climate to use as an example, primarily because it most clearly demonstrates the patterns of beach nourishment–related large-scale shoreline change. Using this extratropical storm–generated wave climate, however, does not result in the greatest magnitudes of shoreline change rates in model experiments without beach nourishment [*Slott et al.*, 2006] or in the greatest magnitudes of nourishment-related shoreline change rates in model experiments with beach nourishment.

6.3. Results

6.3.1. Increased Extratropical Storminess

[34] Figure 6 represents one experiment from the work of *Slott et al.* [2006], in which we subject our initial model shoreline (Figures 6a and 6b) to 200 years of a wave climate altered by an increase in extratropical storm activity (Figure 6, inset, dotted rectangles) versus recent wave climate conditions (Figure 6, inset, solid rectangles), serving as a baseline control model run with no human intervention in the coastal zone. Under recent wave climate conditions (Figure 6c), which are already slightly dominated by extratropical storm–generated waves, the entire cuspate-cape system continues to shift rightward (or rather southwestward if we orient the model shoreline to the regional trend of the Carolina capes), producing shoreline change with an alongshore-averaged absolute magnitude of 1.1 m/yr.

[35] Under increased extratropical storms, the capes accelerate their rightward migration and their plan view shapes become more asymmetric, together causing an increase in alongshore-averaged absolute magnitude of shoreline change to 3.4 m/yr, a roughly threefold increase over shoreline change rates under recent wave climate conditions (Figure 6d). The highest rates of shoreline change concentrate near the cape tips, where rates of recession and accretion individually reach ~6 and ~15 m/yr, respectively, responding to both increased cape migration and the alteration of the large-scale cape shapes. In each of the scenarios, our model conserves the mass of sediment within the nearshore system; the magnitude of shoreline change in accreting areas is balanced by the magnitude of shoreline change in eroding areas.

6.3.2. Increased Extratropical Storminess and Beach Nourishment

[36] We now further examine the case of nourishing at the tip of the cape, while also altering the wave climate driving shoreline evolution. We chose the cape tip as the site of nourishment in the model experiments presented here because they are the most dynamic parts of the cuspate-cape system, responding dramatically to shifts in the wave climate [*Slott et al.*, 2006]. Communities near the tip of one of the Carolina capes also have been some of the most active sites for beach nourishment over the past 65 years [*Valverde et al.*, 1999].

[37] Figure 6e illustrates the results from an experiment nourishing a 10 km stretch of beach and using a wave climate featuring an increase in extratropical storms (Figure 6, inset). The change in shoreline position after 200 years results from two separate forcings: the influence of the wave climate change (Figure 6d, the control run) and the influence of the beach nourishment (Figure 6f, the "human" signal). We computed the influence of beach nourishment in Figure 6f, as highlighted by white- and black-colored bands, by subtracting the shoreline position in Figure 6d from Figure 6e. These two figures represent distinct model runs, as if they existed in distinct universes, using identical initial conditions and wave climates, but in the second model run (Figure 6e) we nourish a 10 km segment of beach.

[38] Shoreline segments in Figure 6f highlighted in white indicate where beach nourishment induced the shoreline to be farther seaward than in the control run; black-highlighted regions indicate where beach nourishment induced the shoreline to be farther landward than in the control run. The areas where the shoreline wound up landward and seaward relative to the control run do not, however, necessarily indicate areas of overall recession or accretion over 200 years. Figure 6f illustrates that white-colored (further seaward due to nourishment) regions generally coincide with eroding areas in Figure 6d and black-colored (further landward) regions generally coincide with areas that accreted in the control run. Localized beach nourishment tended to counteract the effects of the altered wave climate over a long distance in this model run. Figure 6f illustrates that the beach nourishment site itself wound up seaward, relative to the control run, through the net addition of sand as expected. The broad cuspate bay to the left of the nourishment site also wound up seaward, as did much of the cuspate bay to the right of the nourishment site. However, the cape flank downdrift of the nourishment site (Figure 6f, black-colored cape flank) wound up as much as 500 m landward relative to the control run after 200 years.

[39] As a measure of the large-scale effects beach nourishment has on shoreline evolution, we compute the magnitude of shoreline change, expressed as a rate (m/yr): $|r|$, the alongshore average of the absolute magnitude of the difference in shoreline position between the runs with and without beach nourishment within select distances away from the nourishment site. For the experiment depicted in Figure 6f, $|r|$ within 10 km of the nourishment site ($|r_{10}|$), excluding the nourishment site itself, equals 2.4 m/yr, while $|r_{20}|$ (within 20 km) equals 1.4 m/yr. The magnitude of these effects approaches the rate of shoreline change induced by only changing the wave climate (~3 m/yr, Figure 6b) [*Slott et al.*, 2006]. The effects from beach nourishment also spread hundreds of kilometers away from the nourishment area to distances not typically assumed to be directly influenced by nourish-induced gradients in alongshore sediment transport. Although the magnitude of these changes are small compared to the changes tens of kilometers away, the spatially coherent bands of white- and black-colored regions in Figure 6f on adjacent capes indicates the phenomenon is not random, but a systematic effect of the beach nourishment. For example, the black color band approximately 125 km to the left of the beach nourishment site in the cuspate bay (Figure 6f) spans 18 km having an

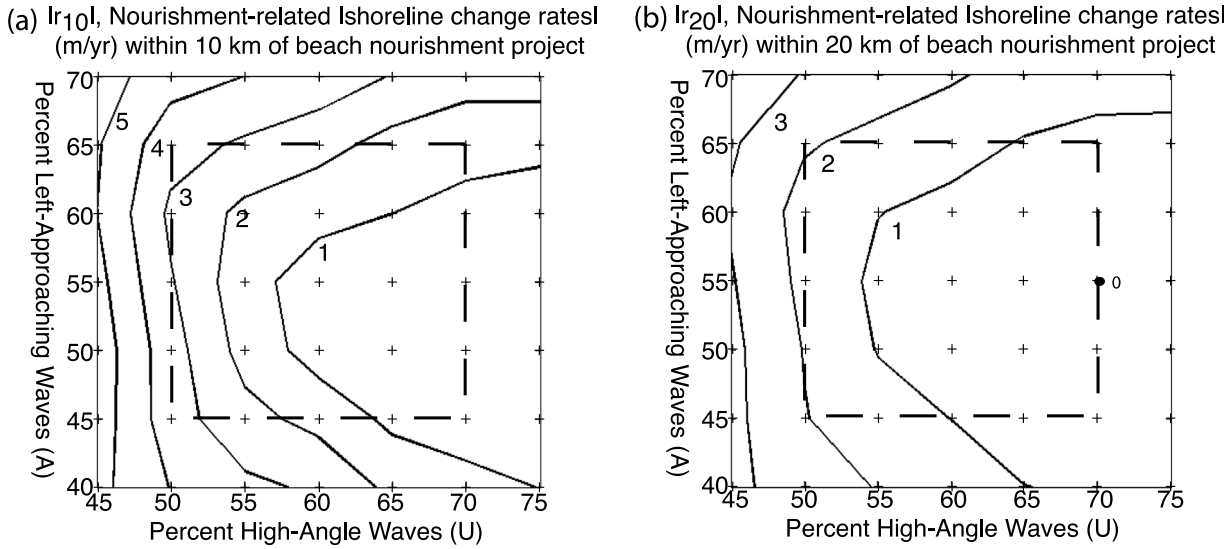

Figure 7. Contour plots of nourishment-caused components of shoreline change rates within (a) 10 km and (b) 20 km of a beach nourishment, excluding the site itself, for different combinations of wave climate parameters A and U (individual model experiments denoted by plus) [*Emanuel*, 1987, 2005; *Slott et al.*, 2006]. Dotted rectangles denote the region where the wave climate parameters change by at most 0.10 and the center of the plot corresponds to an unchanged wave climate ($A = 0.55$, $U = 0.60$). The initial shoreline condition and location of nourishment, a 10 km segment near the tip of a cape, remains the same as in Figure 6.

alongshore-averaged, nourishment-related shoreline change rate of roughly 0.1 m/yr (or 20 m total over 200 years).

6.3.3. Beach Nourishment Under Other Wave Climate Change Scenarios

[40] We also conducted numerous model experiments similar to those depicted in Figure 6 but with different wave climate change scenarios. We explore a set of possible wave climate futures representing 49 possible combinations of wave climate parameters A and U. Figure 7a plots $|r_{10}|$ and Figure 7b plots $|r_{20}|$. Under the WIS Station 509 wave climate (no climate change), $|r_{10}| \sim 0.5$ m/yr and $|r_{20}| \sim 0.3$ m/yr. Decreasing the wave angle highness parameter U corresponding to a relative increase of low-angle waves results in the greatest rates of change. Increasing U, on the other hand, results in negligible widespread effects from beach nourishment at a cape, because increasing the proportion of high-angle waves tends to build capes seaward [*Ashton and Murray*, 2006a], making beach nourishment less necessary at those locations. (Experiments with nourishment located between capes produced a significant effect in these wave climate scenarios, however.) Varying A, the wave climate asymmetry, results in moderate nourishment-related rates of change.

6.3.4. Beach Nourishment Sand Volumes

[41] Figure 8 shows a contour diagram of the quantity of beach sand (expressed as a volumetric rate, i.e., cubic meters of sand per meter alongshore per year) needed to stabilize the position of the 10 km shoreline region over the course of a 200 year simulation (Figure 6). The amount of sand needed to nourish cape-flanking beaches along the Carolina coast may significantly increase if storm patterns change, but these volumes are highly dependent upon the exact nature of the change (Figure 8). Cuspate bays will likely require more intensive shoreline stabilization efforts under wave climate scenarios that feature proportionally more high-angle waves. When the wave climate is influenced by on-shore waves to a greater degree, recession rates at the cape tips increase under the more diffusive wave climate.

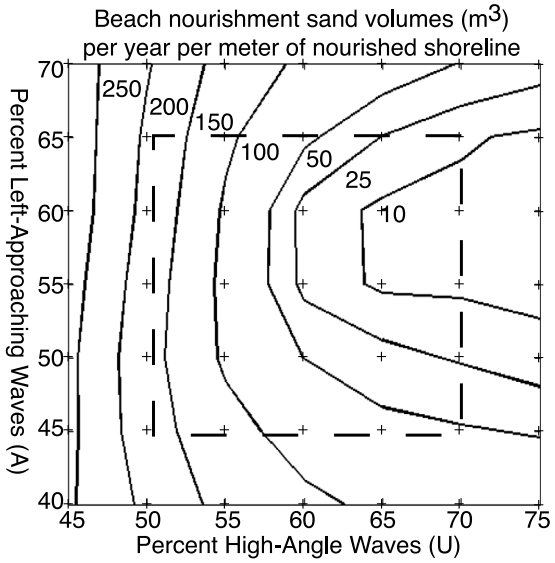

Figure 8. Beach nourishment sand volumes for different combinations of wave climate parameters A and U, as in Figure 7 (individual model experiments denote by plus). Dotted rectangle denotes the region where the wave climate parameters change by at most 0.10 and the center of the plot corresponds to an unchanged wave climate ($A = 0.55$, $U = 0.60$). The initial shoreline condition and location of nourishment, a 10 km segment near the tip of a cape, remains the same as in Figure 6.

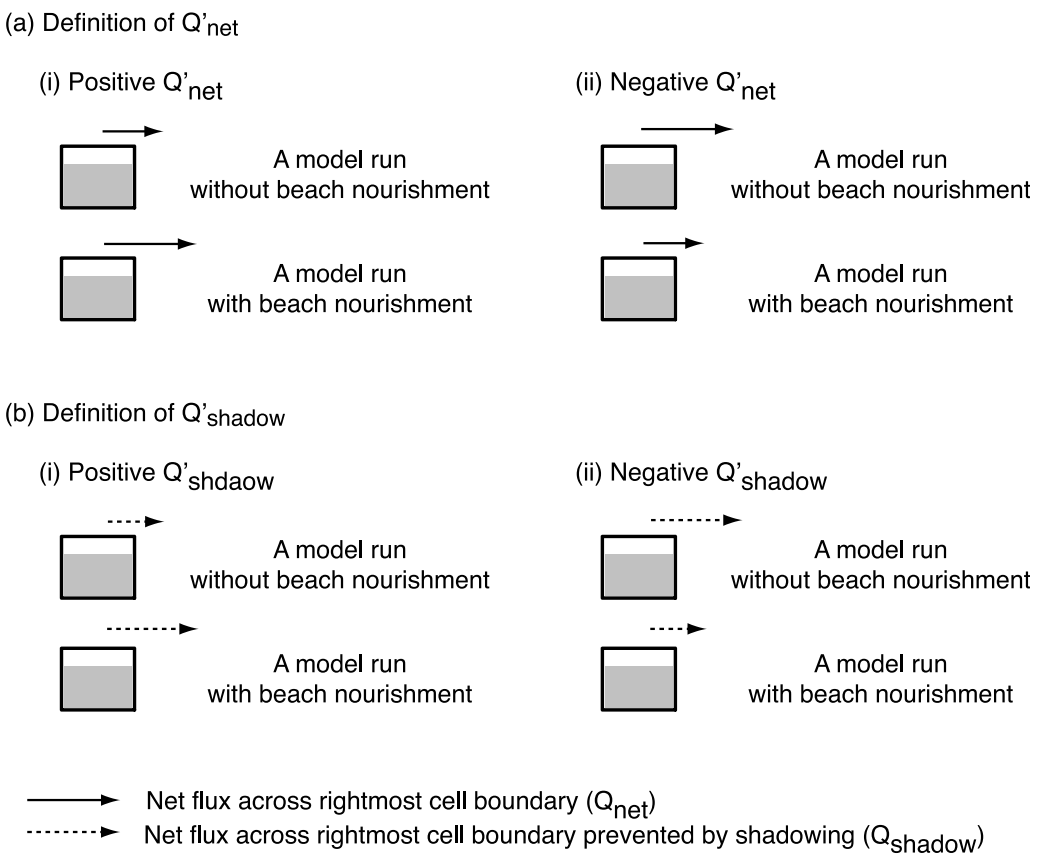

Figure 9. Definition sketch of model run statistics Q_{net}', the flux perturbation, and Q_{shadow}', the flux perturbation caused by wave shadowing.

Under these scenarios, the need for beach nourishment sand to stabilize the position of the cape tip greatly increases (Figure 8). A shift in the directional asymmetry of the wave climate alone (i.e., rightward- versus leftward-directed waves) tends to have a smaller effect on beach nourishment rates.

6.3.5. Interpretation of Physical Mechanisms

[42] As was evident in the experiments involving an initially straight coastline, adjacent beaches may advance for reasons other than beach nourishment sand spreading from the nourished area: adjacent areas may advance because the plan view perturbation in the beach nourishment area induces a convergence of alongshore sediment transport under asymmetric wave climates (e.g., Figures 4, 5, and 6). Beach nourishment, particularly if it occurs near a cape tip, also alters the extent to which protruding features shadow adjacent coastlines from incoming waves and can therefore have a surprisingly long-range effect on other coastal reaches.

[43] We collected two statistics during each model run: the net alongshore sediment transport (Q_{net}) and the influence of wave shadowing on alongshore sediment transport (Q_{shadow}) for each alongshore position in our model domain. We compute the net alongshore sediment transport (Q_{net}) simply as the sum of all fluxes over an entire model run across the right boundary of each shoreline cell, counting rightward-directed fluxes out of the cell as positive. The influence of wave shadowing on alongshore sediment transport (Q_{shadow}) is the sum of all fluxes across the right boundary of each shoreline cell prevented because the cell is shadowed, counting rightward-directed fluxes prevented by wave shadowing out of the cell as positive. These fluxes would have occurred and influenced the evolution of the shoreline if the wave shadowing mechanism did not exist. If a cell is never shadowed, then its Q_{shadow} is zero.

[44] To better understand how beach nourishment induced perturbations to gradients in alongshore sediment transport and wave shadowing, we computed Q_{net}' and Q_{shadow}' as the difference between Q_{net} and Q_{shadow} across the two parallel model runs (a "control" run without beach nourishment and a run with beach nourishment under identical initial model conditions and wave forcing). Figure 9 is a definition sketch that illustrates Q_{net}' and Q_{shadow}' for a hypothetical cell over a model run. In the first two cases (Figures 9a, i and ii), we consider Q_{net}. In the first case (Figure 9a, i), the rightward-directed flux (as represented by solid arrows, where arrow lengths represent relative magnitudes of fluxes) is greater in the model run with beach nourishment than the model run without beach nourishment. In the second case (Figure 9a, ii), the rightward-directed flux is greater in the model run without beach nourishment. In the first case, beach nourishment increases the rightward-directed sediment flux across the two model runs (a positive flux perturbation, Q_{net}'); in the second case, beach nourishment decreases the rightward-directed sediment flux (a negative flux perturbation, Q_{net}') across the two model runs.

[45] Beach nourishment may also induce a change in the extent to which a model cell is shadowed, which is captured by the Q_{shadow}' statistic (Figures 9b, i and ii). In the third case (Figure 9b, i), the model cell is shadowed to a greater

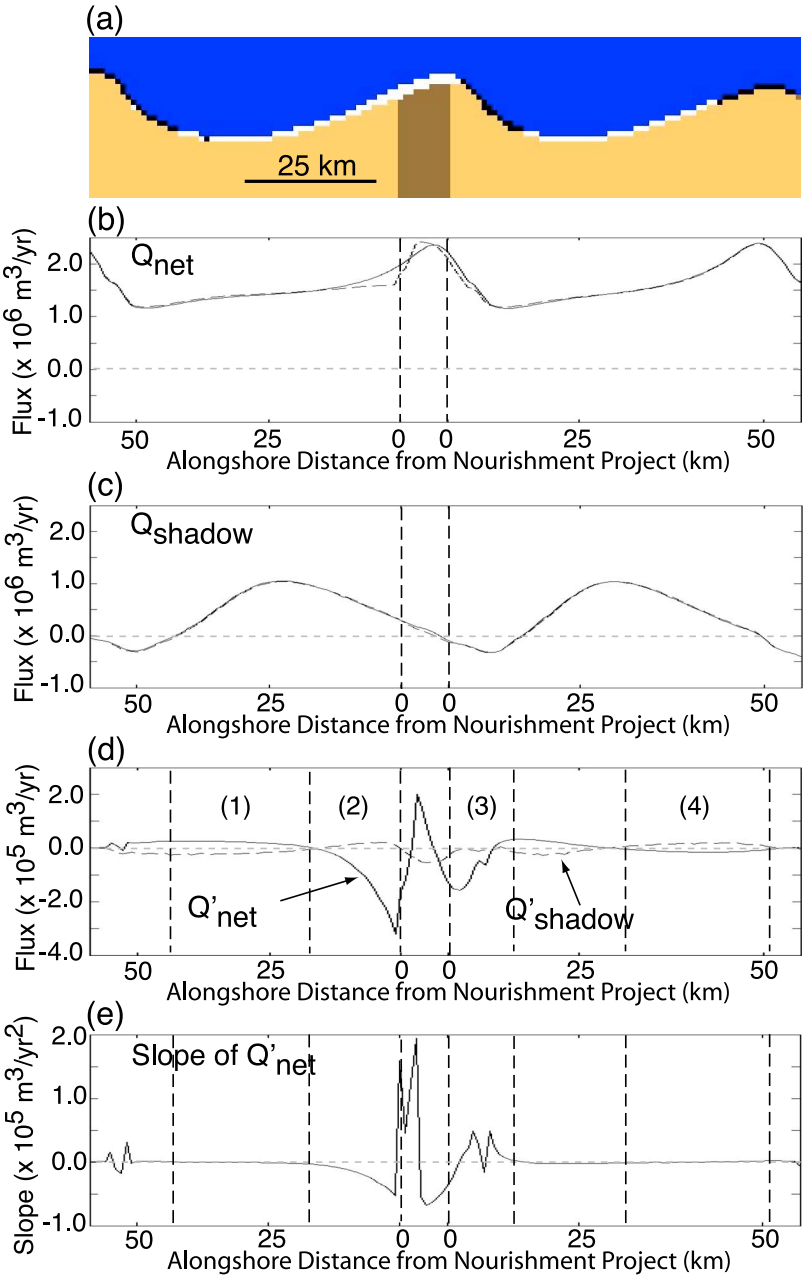

Figure 10. Physical mechanisms of human-induced shoreline change. (a) A magnification of the shoreline region enclosed in the red dotted rectangle from Figure 6f. (b) A plot of Q_{net} for the control model run (solid line) and the model run with beach nourishment (dotted line). (c) A plot of Q_{shadow} for the control model run (solid run) and the model run with beach nourishment (dotted line). (d) The human-induced perturbation to alongshore sediment flux Q_{net}' (solid line), where positive (negative) values indicate an excess of rightward-directed (leftward-directed) flux. The portion of the flux perturbation Q_{shadow}', caused by alterations in wave shadowing, is also plotted (dotted line). (e) Plot of the slope of Q_{net}'.

extent in the model run with beach nourishment than in the model run without beach nourishment, resulting in a positive Q_{shadow}'. In the final case (Figure 9b, ii), the model cell is shadowed to a lesser extent in the model run with beach nourishment than in the model run without beach nourishment, resulting in a negative Q_{shadow}'.

[46] Using Figure 10, which plots Q_{net}' and Q_{shadow}' for a selected region of shoreline from the model run delineated in Figure 6f, we can now explain the mechanism through which nourishment affects shoreline change. We begin with region 1 (Figure 10d), the broad cuspate bay roughly 25–50 km updrift (to the left) of the nourishment area. Nourishing the cape increased the net alongshore sediment transport in the area (positive Q_{net}') caused almost entirely by a decrease in the extent this region was shadowed in the model run with beach nourishment (negative Q_{shadow}'). Spatial gradients in the flux perturbation (Figure 10e, the slope of Q_{net}') correspond to the relative shift in shoreline

position attributed to the beach nourishment activity. The slightly negative slope of Q_{net}' in region 1 represents a convergence of the flux perturbation; the final position of the shoreline winds up farther seaward that it would have otherwise without beach nourishment. The flux convergence induced by beach nourishment is in addition to that induced by the prevailing wave climate absent any forms of human stabilization.

[47] In region 2, the section of coastline updrift of the nourishment area ends up farther seaward because of beach nourishment; the negative slope of the flux perturbation Q_{net}' indicates that beach nourishment induced increased flux convergence. Sediment from the nourishment activity does not accumulate in this region because the net alongshore transport is directed rightward in this area. Rather, by fixing the beach position, nourishment alters the local shoreline angle the nourishment area makes with its neighbors, resulting in the flux convergence. Note that, unlike region 1, the seaward shift of the shoreline occurred despite a net decrease in Q_{net}'. Although wave shadowing is affected in region 2, the change (Q_{shadow}') does not contribute much to the sediment flux perturbation Q_{net}'.

[48] Figure 10 also provides insight into the relative landward shift of the shoreline in region 3, to the right of the nourishment site. The positive slope of the flux perturbation Q_{net}' shows that beach nourishment induces a component of increased flux divergence and further changes to wave shadowing do not play a significant role in the flux perturbation. The flux of sediment across the left boundary of region 3 (Figures 10d, 10e, vertical dotted line) decreases, while the flux of sediment across its right boundary only increases slightly. Cape migration is slowed by the shoreline stabilization, and the sediment that would otherwise have entered region 3 from the left decreased because of altered shoreline angles.

[49] The analysis for region 4 resembles the analysis for region 1: both regions 1 and 4 show wave shadowing plays a key role in spreading the effects from beach nourishment over greater distances, although the magnitudes of the flux perturbations for the adjacent capes are smaller than those adjacent to the nourishment project (regions 2 and 3).

7. Discussion

7.1. Sea Level Rise

[50] In our model experiments, we implicitly assume sea level remains constant. We can expect sea level rise over the coming century to tend to produce a component of recession that will be superimposed on the changes from gradients in alongshore sediment flux that we address. As a rough approximation, we can estimate the sea level component of shoreline change from a geometric conceptual model, where nearshore sediment mass is conserved while the shoreface and barrier island profile shifts upward and landward [*Bruun*, 1962, 1983; *Cowell et al.*, 1995; *Moore et al.*, 2007; *Stolper et al.*, 2005; *Wolinsky and Murray*, 2009]. The rate of shoreline retreat in such models is sensitive to the geometry assumed for the profile, determined by the landward and seaward limits of wave-driven sediment transport. In such models, the component of shoreline retreat rate related to sea level rise is the sea level rise rate multiplied by the inverse of the average slope of the active profile. The geometry of active profiles varies spatially and depends on the time scales involved [*Stive et al.*, 1991]. Over short time scales, the slope of the upper shoreface, approximately 0.01, is often considered the relevant part of the profile [*Bruun*, 1962; *Zhang et al.*, 2004]. On time scales longer than the typical return intervals of large storms, the entire composite barrier island and shoreface profile must be considered, giving a slope that can be considerably lower. For a specific part of the northern outer banks of North Carolina, this slope is approximately 0.0015 [*Moore et al.*, 2007]. Thus, depending on time scales and assumptions of geometry, estimates of the component of shoreline retreat caused by sea level rise can vary widely, and comparisons between the effects of human manipulations and sea level rise can only be order-of-magnitude estimates. Using the commonly assumed 0.01 slope [*Zhang et al.*, 2004], sea level rise may contribute roughly 0.48 m/yr of shoreline recession, assuming a sea level rise of 0.48 m over the coming century [*Intergovernmental Panel on Climate Change*, 2007]. (Using the longest-term assumptions for the profile geometry (i.e., a slope of approximately 0.0015), the estimated retreat rate would be a few meters per year.) As demonstrated by *Slott et al.* [2006], the rate at which the shoreline erodes or accretes because of moderate changes in storm patterns can reach nearly an order of magnitude larger than this 0.48 m/yr estimate of sea level rise recession rate. The results we present here suggest that the component of shoreline change induced by nourishment, tens of kilometers away from a nourishment site, even if prevailing wave climates persist into the future, are also commensurate with the range of estimates for the sea level rise component and may, under many of the possible wave climate futures (Figure 7), be greater.

7.2. Model Simplifications

[51] "One-contour-line"-based coastline models, including ours, make simplifying assumptions, omitting many smaller-scale sediment transport processes and features specific to the Carolina coast and cuspate-cape coastlines in general.

7.2.1. Wave Transformation

[52] We ignore wave diffraction or complex refraction that takes places at the cape tips. We also ignore the effects nonshore-parallel shoreface contours have on wave refraction [*Falqués and Calvete*, 2005; *McNinch*, 2004; *List and Ashton*, 2007]. *Falqués and Calvete* [2005] demonstrated that for shorelines with undulations of sufficiently large alongshore-wavelength (>~10 km) the high-angle wave instability mechanisms holds over a robust set of wave and shoreface parameters. As a simplification, our model shoals and refracts waves assuming shore-parallel contours extend to the WIS station depth (215 m) from which our two wave climate parameters (A and U) were derived. A more realistic wave shoaling and refraction routine that instead considers deviations from shore-parallel contours would compute different wave-breaking quantities (H_b, ϕ_b) than in our model runs, especially for longer-period waves that interact significantly with the bottom in depths greater than the base of the shoreface. Because we calibrated our control model run (with no beach nourishment and prevailing wave climate conditions) to match the maximum rates of change observed on our case study coastline [*Slott et al.*, 2006], we would correspondingly expect to recalibrate K in equation (2), also.

Alternatively, we could derive the wave climate parameters from WIS stations closer to the shoreline [*Ashton and Murray*, 2006b] so that the contours between that location and the shoreline would be approximately shore parallel on large scales. However, these stations will not provide a regional wave climate free from the influence of wave shadowing from adjacent capes [*Ashton and Murray*, 2006b].

7.2.2. Sediment Availability

[53] We assume at least a thin veneer of sediment covers the shoreface at all times; bedrock outcrops on natural shorefaces can limit the amount of mobile sediment and constrain alongshore sediment fluxes [*Valvo et al.*, 2006]. This study addresses sandy coastlines; the response of other types of coastlines (e.g., rocky) to climate change and beach nourishment may differ [*Dickson et al.*, 2006]. We also assume the process of sand extraction used for nourishment does not affect the shoreline; for example, we ignore any effects dredging nourishment sand from ebb tidal shoals or the deeper portions of the shoreface has on the dynamics of shoreline system. The model does not consider the impoundment of alongshore-transported sediment in extensive shoals extending from the capes [*McNinch and Leuttich*, 2000; *McNinch and Wells*, 1999].

7.2.3. Wave Height Gradients

[54] An alternative formulation for alongshore sediment transport Q adds the influence of local gradients in alongshore wave height to the standard CERC equation. Most of these formulations follow the general form derived by *Ozasa and Brampton* [1980], such as the one presented by *Horikawa* [1988] and used by *Falqués and Calvete* [2005]:

$$Q = \mu H_b^{5/2}\left(\sin(2\alpha_b) - \frac{2r}{\beta}\cos(\alpha_b)\frac{\partial H_b}{\partial x}\right). \quad (4)$$

[55] We can evaluate the effect the wave height gradient term ($\frac{2r}{\beta}\cos(\alpha_b)\frac{\partial H_b}{\partial x}$) has on alongshore sediment transport by computing Q as follows. Observing that the shoreline angle between adjacent cells on our case study cuspate-cape coastline ($\partial\theta/\partial x$) is generally very small (Figure 11a), we compute breaking wave angles (α_b) and heights (H_b) by shoaling and refracting deepwater waves as we do in our model runs for three different scenarios, when $\partial\theta/\partial x = 2°$, 4°, and 10° per kilometer (the scale of spatial discretization). For each demonstration scenario, we compute Q for all integer deepwater wave angles (α_0) (Figures 11b, 11c, and 11d) by substituting $r = 1.0$ (nondimensional constant), $\beta = 0.01$ (beach slope), and use a typical value of 0.15 $m^{1/2}\ s^{-1}$ for μ [*Falqués and Calvete*, 2005].

[56] The influence the wave height gradient term has on Q is generally small for most combinations of values of $\partial\theta/\partial x$ and α_0 (Figures 11b and 11c). Surprisingly, when including the wave height gradient term, the maximum alongshore sediment flux could occur for a deepwater angle smaller than for the standard CERC equation (e.g., Figure 11b). As a result, we would expect the diffusivity of model wave climates to diminish (or for antidiffusivity to be enhanced, if the climate is dominated by high-angle waves). Nevertheless, the simple example presented here demonstrates that including a wave height gradient term in the CERC equation would have little effect on model results for the large spatial scales (hundreds of kilometers of domain with 1000 m cells) we consider.

7.2.4. Shifts in Wave Climates

[57] The model treats only instantaneous shifts in wave climates, rather than shifts which develop gradually over the course of decades. When formulating wave climate scenarios for possible future changes in warming-induced storminess, we ignore the effect varying storm activity has on average wave height, representing shifts in the angular distribution of approaching waves only. (This simplification suggests that we may be underestimating (overestimating) the effects from increased (decreased) storm activity on shoreline change, because an increase (decrease) in storminess will also increase (decrease) average wave heights.) Our future wave climate scenarios are themselves order-of-magnitude approximations, recognizing the imperfect state of the science surrounding the link between storm activity and global warming [*Donnelly and Woodruff*, 2007; *Emanuel*, 2005, 1987; *Lambert*, 1995; *Landsea*, 2005; *Pielke*, 2005; *Webster et al.*, 2005]. (Recent evidence also indicates that wave climates felt along the Carolina coast during the past 30 years have already been influenced by altered storm patterns [*Komar and Allan*, 2007].)

7.2.5. Model Insights

[58] An initial comparison of nourishment sand volumes (section 6.3.4) to past nourishment practices along the Carolina coast (Appendix A) suggests we are not unrealistically driving shoreline evolution by adding too much sand in our model experiments. Also, the quantitative output of our model experiments depend upon the choice of several poorly constrained model parameters (e.g., time interval between nourishment episodes, alongshore length of nourishment stretches). Further experiments show that varying some of the key model parameters over reasonable ranges does not significantly affect the results we have presented in this paper, however (Appendix B).

[59] Given these simplifications, our model results are not meant to be quantitatively reliable predictions. Nevertheless, these model experiments let us estimate the relative influence that three primary drivers (shifts in storminess-related wave climates, direct human modifications to the shoreline system, and sea level rise) have on shoreline evolution on time and spatial scales much greater than are traditionally considered when nourishment effects are analyzed. When considering the consequences of beach nourishment on shoreline migration, coastal managers and scientists implicitly assume the effects always result in adjacent shorelines migrating seaward [*Dean*, 2002]. Our work here demonstrates that this is not always true, particularly when we take into account the large-scale shape and orientation of the shoreline, the influence of high-angle waves, and the role that wave shadowing plays in rapidly transmitting the effects of human stabilization on shoreline evolution over large spatial scales. Although sea level rise garners much attention from coastal communities, their direct actions to stabilize disappearing beaches may induce effects just as significant as the ones they are meant to combat. By casting direct human manipulations (i.e., beach nourishment) of the shoreline into our large-scale modeling framework, we can begin to gain an understanding of the complex and nonlocal nature of the shoreline response.

[60] Although we include human actions in our modeling process, we do not explicitly include the dynamical nature of their decision-making process. In practice, beach nour-

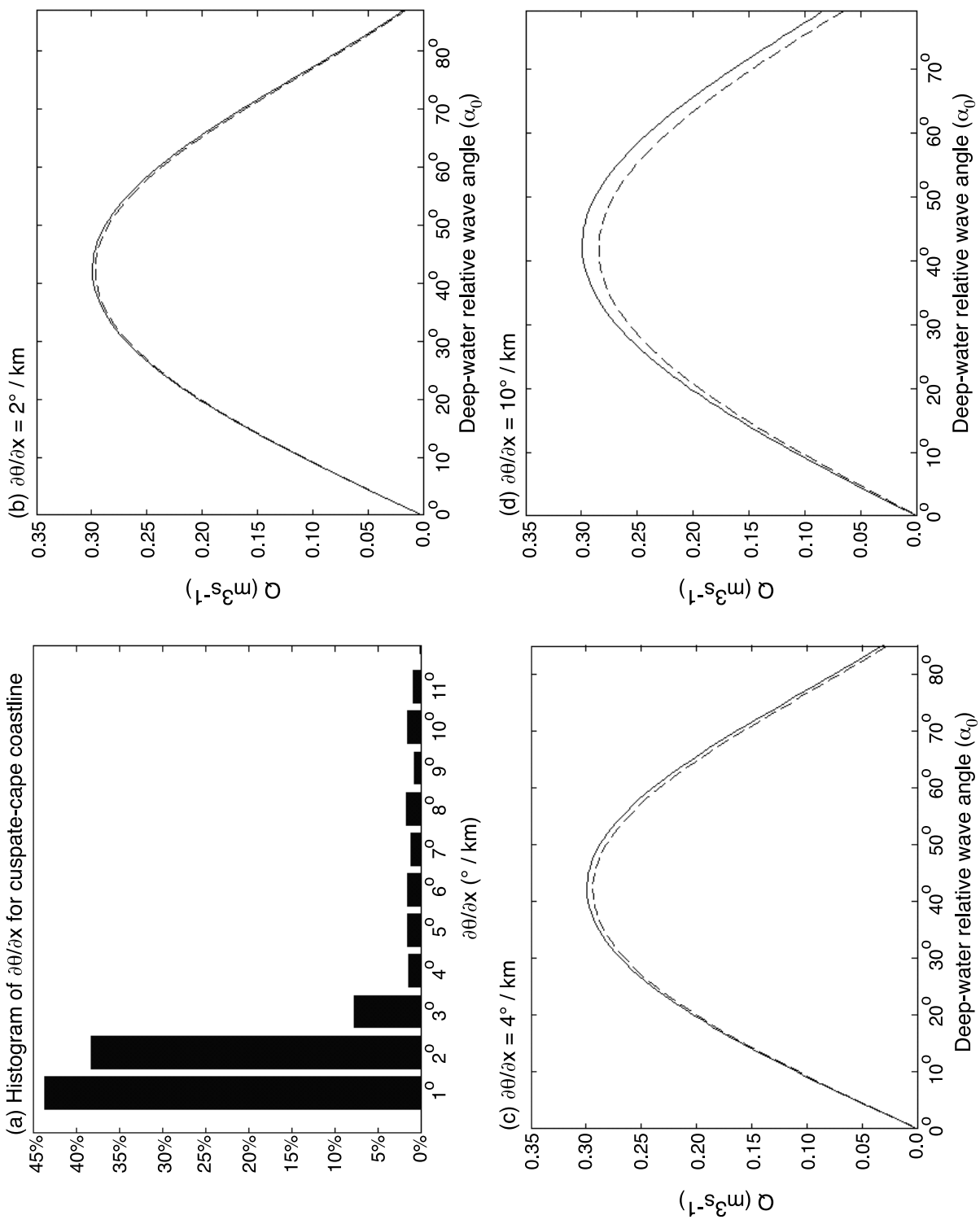
(a) Histogram of ∂θ/∂x for cuspate-cape coastline
∂θ/∂x (° / km)
(b) ∂θ/∂x = 2° / km
(c) ∂θ/∂x = 4° / km
(d) ∂θ/∂x = 10° / km
Q (m³s⁻¹)
Deep-water relative wave angle (α0)
CERC
CERC + ∂H/∂x term

Figure 11

Table 1. Sensitivity of Model Results to Changes in Beach Nourishment Interval I for Conditions Used in Figure 6e

I	$\lvert r_{10}\rvert$ (±change) (m/yr)	$\lvert r_{20}\rvert$ (±change) (m/yr)
1 day	2.4	1.4
3 years	2.3 (−0.1)	1.3 (−0.1)
5 years	2.2 (−0.2)	1.3 (−0.1)
10 years	2.1 (−0.3)	1.2 (−0.2)

Table 2. Sensitivity of Model Results to Beach Nourishment Length L

L	$\lvert r_{10}\rvert$ (±change) (m/yr)	$\lvert r_{20}\rvert$ (±change) (m/yr)
10 km	2.4	1.4
7 km	2.6 (+0.2)	1.6 (+0.2)
5 km	2.8 (+0.4)	1.9 (+0.5)

ishment activity is not static as we have modeled here; the decision to begin nourishing a beach depends upon a more complex set of conditions beyond the mere condition that the beach has eroded beyond some "initial" location. Typically, communities conduct an economic, cost-benefit analysis of proposed beach nourishment; a favorable outcome to such an analysis is required to receive federal matching funds [*U.S. Congress*, 1986]. Dynamic capital theory allows us to explore the nature of human, economic decisions in a highly stylized, single-dimension model of beach nourishment [*Smith et al.*, 2009]. By coupling this model to our spatially extended model of the morphodynamic response of coastlines to beach nourishment, we may observe new, emergent behaviors.

8. Conclusions

[61] Despite commonly held notions, the effect of beach nourishment on adjacent shoreline segments cannot always be adequately described using a linear shoreline diffusivity. On a straight shoreline, nourishing a single segment of beach under diffusive wave climates causes adjacent shoreline areas to advance, whereas under antidiffusive (or neutrally diffusive) wave climates, adjacent shoreline areas may both advance and retreat. Under diffusive wave climate regimes, adjacent shoreline areas advance regardless of any prevailing directional asymmetry of the wave climate.

[62] On complex-shaped coastlines similar to those found in nature (e.g., cuspate-capes), these varied morphological responses manifest themselves as we select different positions along the coastline to nourish. As we repeatedly nourish near the tip of a cape, pinning it in place, the downdrift flank tends to move landward in response (relative to the case without nourishment). The effect on shoreline evolution of nourishing toward the cuspate bays more resembles the classic diffusion of shoreline shape. In other areas, where the natural migration of the large-scale coastline shapes results in very little retreat, beach nourishment is barely needed and has little effect. The volume of beach nourishment sediment needed to maintain a shoreline location may vary by up to 2 orders of magnitude depending on the location of nourishment along the cuspate coast.

[63] Finally, altering the wave climate to explore the global warming–induced changes we might expect over the coming century, we find that the human-induced component of shoreline change may be on the same order of magnitude as the change induced by sea level rise. Model runs suggest that these long-term effects may spread on the order of tens of kilometers away from the nourishment area itself.

[64] As a result of humans' intentional interference with the natural evolution of coastlines over the past several decades, few coastlines can be considered pristine. Human interference in the coastal zone will likely intensify in the future. As in many human-natural coupled landscape systems [*McNamara and Werner*, 2008a, 2008b], human and natural forces must be considered together when understanding the morphological evolution of developed coastline systems.

Appendix A: Initial Comparison of Model Nourishment Sand Volumes to Past Nourishment Practices

[65] We can make some initial comparisons from the model run which uses recent wave climate conditions (A = 0.55, U = 0.60; *WIS*) to past nourishment practices. Along the North Carolina coastline, Wrightsville Beach and Carolina Beach have both nourished their beaches at regular intervals over the past roughly half-century and continue to do so today [*Valverde et al.*, 1999; Beach nourishment histories are catalogued by the Program for the Study of Developed Shorelines, found at http://www.wcu.edu/1037.asp, hereafter *PSDS*] and furthermore occupy the approximate position relative to their cape tips (i.e., Cape Lookout, NC) that the beach nourishment site selected for our model experiments in Figure 6 does. Beach nourishment at these two sites represents nearly 40% (volumetrically) of the total beach nourishment activity in North Carolina over the past 65 years [*PSDS*]. Under recent wave climate conditions, the model run placed nearly 18 m^3 per meter of shoreline per year. Projects at the two North Carolina locations have nourished at roughly 5–10 times this rate over the past 50 years (~90 m^3/m/yr at Wrightsville Beach and ~163 m^3/m/yr at Carolina Beach) [*Valverde et al.*, 1999]. (Past beach nourishment data for these two locations are, unfortunately, incomplete: in many cases, either the alongshore length (m) of nourished beach or total sand volume placed (m^3), or both, are unavailable. For both locations, however, we simply take the average of fully documented sand volumes and lengths to compute the volumetric rate of beach nourishment sand placement.)

[66] As a further comparison, the U.S. Army Corps of Engineers planned a 50 year, nearly continuously recurring beach nourishment project along two segments of

Figure 11. Influence of wave height gradients term on Q. (a) Histogram of angles between adjacent cells (1 km wide), $\partial\theta/\partial x$, for our case study (Figure 6). The larger values are found exclusively at the cape tips. (b) Plot of Q using the standard CERC equation (solid line) (equation (4) without the wave height gradient term) versus an alternative formulation that considers gradients in alongshore wave height (broken line) (equation (4)), assuming the angle between adjacent shoreline cells is 2°. (c) Plot similar to Figure 11b, assuming the angle between adjacent shoreline cells is 4°. (d) Plot similar to Figure 11b, assuming the angle between adjacent shoreline cells is 10°.

coastline in Dare Country, NC, USA [*USACE*, 2002]. After an initial construction phase, the expected recurring nourishment volume required to pin the north and south shoreline segments in place over the long term more closely resembles model nourishment volumes: using a value of D = 27 ft (8.23 m), 30.5 m^3/m/yr is projected to be required for the northern region (2,167,513 m^3 per 23.7 km per 3 years) and 16.0 m^3/m/yr for the southern region (806,605 m^3 per 16.8 km per 3 years).

Appendix B: Sensitivity to Model Parameters

[67] We conducted additional model runs that test the sensitivity of our results to certain input model parameters. In the model runs presented here, we nourish the selected shoreline segments at every time step (i.e., 1 day), if they have eroded beyond their initial position, achieving the desired modeling goal of pinning the shoreline in place over the long-term. In practice, beach nourishment typically only takes place every several years, so we test the sensitivity of our model results to our simplifying model assumption. We repeat our model runs while varying only the interval at which we conduct beach nourishment. We test three additional beach nourishment intervals I (I = 3, 5, and 10 simulated years) and find that changing this parameter does not significantly affect model results (Table 1).

[68] We also tested the model's sensitivity to our choice of a 10 km beach nourishment length, because this value exceeds most historical beach nourishment lengths, instead using lengths of L = 5 km and L = 7 km, while keeping all other model parameters the same; changes in L have only minor effects upon the results (Table 2). (Although historical lengths have tended to be smaller than 10 km, recent trends suggest longer beach nourishment projects may become typical [*Valverde et al.*, 1999]. A single 50 year beach nourishment project planned for Dare County, NC, spans 28 km, for example [*USACE*, 2002].)

[69] All model run results embody some element of random probability. When we conduct duplicate model experiments forced by waves selected from the wave climate PDF using a different random number generator seed (ref. section 3.2), we observe that rates of geomorphic change on the coastline vary by ±0.1 m/yr on average, and within an order of magnitude of the model's sensitivity to varying other parameters, I and L. This suggests that the model's sensitivity to these other parameters is not easily distinguishable from the stochasticity of wave climate draws. Only when $L \leq 5$ km did the changes in the rates of shoreline change significantly exceed the lower-bound threshold value.

[70] **Acknowledgments.** The National Science Foundation (DEB 0507987) and the Duke University Center on Global Change supported this work. We thank Laura Moore for reviewing an earlier draft of this paper.

References

Ashton, A. D., and A. B. Murray (2006a), High-angle-wave instability and emergent shoreline shapes: 1. Modeling of sandwaves, flying spits, and capes, *J. Geophys. Res.*, *111*, F04011, doi:10.1029/2005JF000422.

Ashton, A. D., and A. B. Murray (2006b), High-angle-wave instability and emergent shoreline shapes: 2. Wave climate analysis and comparisons to nature, *J. Geophys. Res.*, *111*, F04012, doi:10.1029/2005JF000423.

Ashton, A. D., A. B. Murray, and O. Arnoult (2001), Formation of coastline features by large-scale instabilities induced by high-angle waves, *Nature*, *414*, 296–300.

Bruun, P. (1962), Coastal erosion and the development of beach profiles, *J. Waterw. Harbors Div. Am. Soc. Civ. Eng.*, *88*, 117–130.

Bruun, P. (1983), Review of conditions for uses of the Bruun Rule of erosion, *Coastal Eng.*, *7*, 77–89.

Cowell, P. J., P. S. Roy, and R. Jones (1995), Simulation of large-scale coastal change using a morphological behaviour model, *Mar. Geol.*, *126*, 45–61.

Dean, R. G. (1991), Equilibrium beach profiles: Characteristics and applications, *J. Coastal Res.*, *7*(1), 53–84.

Dean, R. G. (2002), *Beach Nourishment: Theory and Practice*, World Sci., Hackensack, N. J.

Dean, R. G., and C.-H. Yoo (1992), Beach-nourishment performance predictions, *J. Waterw. Port Coastal Ocean Eng.*, *118*(6), 567–586.

Deigaard, R., J. Fredsoe, and I. B. Hedegaard (1988), Mathematical model for littoral drift, *J. Waterw. Port Coastal Ocean Eng.*, *112* (3), 351–369.

Dickson, M. E., M. J. A. Walkden, and J. W. Hall (2006), Systemic impacts of climate change on an eroding coastal region over the twenty-first century, *Clim. Change*, *84*, 141–166, doi:10.1007/s10584-006-9200-9.

Donnelly, J. P., and J. D. Woodruff (2007), Intense hurricane activity over the past 5,000 years controlled by El Niño and the West African monsoon, *Nature*, *447*, 465-468, doi:10.1038/nature05834.

Emanuel, K. A. (1987), The dependence of hurricane intensity on climate, *Nature*, *326*, 483–485.

Emanuel, K. A. (2005), Increasing destructiveness of tropical cyclones over the past 30 years, *Nature*, *436*, 686–688.

Falqués, A., and D. Calvete (2005), Large-scale dynamics of sandy coastlines: Diffusivity and instability, *J. Geophys. Res.*, *100*, C03007, doi:10.1029/2004JC002587.

Haff, P. K. (2007), The landscape Reynolds number and other dimensionless measures of Earth surface processes, *Geomorphology*, *91*, 178–185, doi:10.1016/j.geomorph.2007.04.010.

Hanson, H., and N. C. Kraus (1989), *GENESIS: Generalized Model for Simulating Shoreline Change, Report 1: Technical Reference*, U.S. Army Eng. Waterw. Exp. Stn., Coastal Eng. Res. Cent., Vicksburg, Miss.

Hooke, R. G. (1994), On the efficacy of humans as geomorphic agents, *GSA Today*, *4*(9), *217*, 224–225.

Hooke, R. G. (2000), On the history of humans as geomorphic agents, *Geology*, *28*(9), 843–846.

Horikawa, K. (1988), *Nearshore Dynamics and Coastal Processes*, Univ. of Tokyo Press, Tokyo.

Intergovernmental Panel on Climate Change (2007), *Climate Change 2007: Impact, Adaptation, and Vulnerability—Contribution of Working Group II to the Fourth Assessment Report of the Intergovernmental Panel on Climate Change*, Cambridge Univ. Press, New York.

James, L. A., and W. A. Marcus (2006), The human role in changing fluvial systems: Retrospec, inventory and prospect, *Geomorphology*, *76*, 152–171.

Komar, P. D. (1971), The mechanics of sand transport on beaches, *J. Geophys. Res.*, *76*, 713–721, doi:10.1029/JC076i003p00713.

Komar, P. D. (1998), *Beach Processes and Sedimentation*, Simon and Schuster, Upper Saddle River, N. J.

Komar, P. D., and J. C. Allan (2007), Higher waves along U.S. East Coast linked to hurricanes, *Eos Trans. AGU*, *88*(30), 301–308.

Komar, P. D., and D. L. Inman (1970), Longshore sand transport on beaches, *J. Geophys. Res.*, *75*, 5914–5927, doi:10.1029/JC075i030p05914.

Lambert, S. J. (1995), The effect of enhanced greenhouse warming on winter cyclone frequencies and strengths, *J. Clim.*, *8*, 1447–1452.

Landsea, C. W. (2005), Hurricanes and global warming, *Nature*, *438*, E11–E13.

Larson, M., N. C. Kraus, and M. R. Byrnes (1990), SBEACH: Numerical model for simulating storm-induced beach change: Report 2. Numerical formulation and model tests, *Tech. Rep. CERC-89-9*, U. S. Army Eng. Waterw. Exp. Stn., Coastal Eng. Res. Cent., Vicksburg, Miss.

List, J. H., and A. D. Ashton (2007), A circulation modeling approach for evaluating the conditions for shoreline instabilities, in *Coastal Sediments '07*, edited by N. C. Kraus and J. D. Rosati, pp. 327–340, Am. Soc. of Civ. Eng., New Orleans, La.

McNamara, D., and B. Werner (2008a), Coupled barrier island-resort model: 1. Emergent instabilities induced by strong human-landscape interactions, *J. Geophys. Res.*, *113*, F01016, doi:10.1029/2007JF000840.

McNamara, D. E., and B. T. Werner (2008b), Coupled barrier island-resort model: 2. Tests and predictions along Ocean City and Assateague

Island National Seashore, Maryland, *J. Geophys. Res.*, *113*, F01017, doi:10.1029/2007JF000841.
McNinch, J. E. (2004), Geologic control in the nearshore: shore-oblique sandbars and shoreline erosional hotspots, Mid-Atlantic Bight, USA, *Mar. Geol.*, *211*, 121–141.
McNinch, J. E., and R. A. Leuttich (2000), Physical processes around a cuspate foreland headland: Implications to the evolution and long-term maintenance of a cape-associated shoal, *Cont. Shelf Res.*, *20*, 2367–2389.
McNinch, J. E., and J. T. Wells (1999), Sedimentary processes and depositional history of a cape-associated shoal, Cape Lookout, North Carolina, *Mar. Geol.*, *158*, 233–252.
Moore, L., J. H. List, S. J. Williams, and D. Stolper (2007), Modeling barrier island response to sea level rise in the Outer Banks, North Carolina, in *Coastal Sediments '07*, edited by N. C. Kraus and J. D. Rosati, pp. 1153–1164, Am. Soc. Civ. Eng., New Orleans, La.
Ozasa, H., and A. H. Brampton (1980), Mathematical modeling of beaches backed by seawalls, *Coastal Eng.*, *4*(1), 47–64.
Pielke, R. A., Jr. (2005), Are there trends in hurricane destruction?, *Nature*, *438*, E11.
Pilkey, O. H., W. J. Neal, S. R. Riggs, C. A. Webb, D. M. Bush, D. F. Pilkey, J. Bullock, and B. A. Cowan (1998), *The North Carolina Shore and its Barrier Islands*, Duke Univ. Press, Durham, N. C.
Reolvink, J. A., and G. K. F. M. Van Banning (1994), Design and development of Delft3D and application to coastal morphodynamics, paper presented at Hydroinformatics '94 conference, Delft, Netherlands.
Slott, J. M., A. B. Murray, A. D. Ashton, and T. J. Crowley (2006), Coastline responses to changing storm patterns, *Geophys. Res. Lett.*, *33*, L18404, doi:10.1029/2006GL027445.
Smith, M. D., J. Slott, D. McNamara, and A. B. Murray (2009), Beach nourishment as a dynamic capital accumulation problem, *J. Environ. Econ. Manage.*, *58*, 58–71, doi:10.1016/j.jeem.2008.07.01.
Stive, M. J. F., et al. (1991), Sea-level rise and shore nourishment – A discussion, *Coastal Eng.*, *16*(1), 147–163.
Stolper, D., J. H. List, and E. R. Thieler (2005), Simulating the evolution of coastal morphology and stratigraphy with a new morphological-behaviour model (GEOMBEST), *Mar. Geol.*, *218*, 17–36, doi:10.1016/j.margeo.2005.02.019: 17–36.
Syvitski, J. P. M., C. J. Vörösmarty, A. J. Kettner, and P. Green (2005), Impact of humans on the flux of terrestrial sediment to the global coastal ocean, *Science*, *308*, 376–380, doi:10.1126/science.1109454.
U.S. Army Corps of Engineers (2002), *Final feasibility report and environmental impact statement on hurricane protection and beach erosion control: Dare Country beaches*, vol. 1, Wilmington District, South Atlantic Division, Dare County, N. C.
U.S. Congress (1986), Water Resources Development Act of 1986, *Public Law 99-662*, 99th Congress.
Valverde, H. R., A. C. Trembanis, and O. H. Pilkey (1999), Summary of beach nourishment episodes on the U.S. East Coast Barrier Islands, *J. Coastal Res.*, *15*, 1100–1118.
Valvo, L., A. B. Murray, and A. Ashton (2006), How does underlying geology affect coastline change? An initial modeling investigation, *J. Geophys. Res.*, *111*, F02025, doi:10.1029/2005JF000340.
Webster, P. J., G. J. Holland, J. A. Curry, and H.-R. Chang (2005), Changes in tropical cyclone number, duration, and intensity in a warming environment, *Science*, *309*, 1844–1846.
Werner, B., and D. McNamara (2007), Dynamics of coupled human landscape systems, *Geomorphology*, *91*, 393–407.
Wolinsky, M., and A. B. Murray (2009), A unifying framework for shoreline migration: 2. Application to wave-dominated coasts, *J. Geophys. Res.*, *114*, F01009, doi:10.1029/2007JF000856.
Zhang, K. Q., B. C. Douglas, and S. P. Leatherman (2004), Global warming and coastal erosion, *Clim. Change*, *64*, 41–58.

A. D. Ashton, Geology and Geophysics Department, Woods Hole Oceanographic Institution, 360 Woods Hole Rd., MS-22, Woods Hole, MA 02543, USA.

A. B. Murray and J. M. Slott, Division of Earth and Ocean Sciences, Nicholas School for the Environment and Earth Sciences, Center for Nonlinear and Complex Systems, Duke University, Box 90229, Durham, NC 27708-0227, USA. (jordan.slott@duke.edu)